



Enhancement of positron annihilation on molecules due to vibrational Feshbach resonances

G.F. Gribakin

Department of Applied Mathematics and Theoretical Physics, Queen's University, Belfast BT7 1NN, Northern Ireland, UK

Abstract

The zero-range potential model is used to investigate positron collisions and annihilation with molecules. The Kr_2 dimer is considered as an example. It is shown that (i) although positrons do not bind to individual Kr atoms, they do form bound states with Kr_2 . (ii) A sequence of vibrationally excited states of the positron–molecule complex extends into the positron continuum, where it manifests as vibrational Feshbach resonances. (iii) These resonances give a very large contribution to the positron annihilation rate. Even after averaging over the thermal positron energy distribution, the contribution of the lowest Feshbach resonance exceeds that of the non-resonant background by an order of magnitude. © 2002 Elsevier Science B.V. All rights reserved.

PACS: 34.50.-s; 78.70.Bj; 71.60.+z; 36.10.-k

1. Introduction

The aim of this paper is to show that when low-energy positrons collide with molecules they can be captured in vibrational Feshbach resonances, which leads to strong enhancement of the positron annihilation rate.

It has been known for about 50 years that positron annihilation rates in many polyatomic molecular gases are extremely large [1–6]. This fact is most obvious when one expresses the positron annihilation rate λ in terms of an effective number of electrons, Z_{eff} , which contribute to the annihilation on a given atom or molecule [7],

$$\lambda = \pi r_0^2 c Z_{\text{eff}} n, \quad (1)$$

where n is the number density of the gas, r_0 is the classical electron radius and c is the speed of light. The value of Z_{eff} for many molecules is much higher than the actual number of electrons in the molecule, in some cases by up to five orders of magnitude, e.g. for anthracene $\text{C}_{14}\text{H}_{10}$, $Z_{\text{eff}} = 4.3 \times 10^6$ [8]. It also displays a very rapid increase with the size of the molecule, e.g. for hydrocarbons $\text{C}_n\text{H}_{2n+2}$, $Z_{\text{eff}} \propto n^6$ [6,9]. Such an increase is just one manifestation of strong chemical sensitivity of Z_{eff} .

There are two main effects which enhance Z_{eff} [9,10]. The first one, originally considered in [11], operates when the positron has a low-lying virtual or weakly bound state with the target. This causes an enhancement of the positron density near the molecule, thereby increasing the annihilation rate. Note that this increase is matched by a similar increase of the elastic scattering cross-section [12]. This type of enhancement may take place for both

E-mail address: g.gribakin@am.qub.ac.uk (G.F. Gribakin).

atoms and molecules. In particular, it is responsible for large values of Z_{eff} in heavier noble-gas atoms [13–15].

The second mechanism which operates for molecules only involves capture of the positron into a (quasi)bound positron–molecule state. It was often assumed that such process might be behind the anomalously large annihilation rates [5,16–18]. However, the details of this mechanism are only becoming clear now [9,10]. In particular, it seems certain that low-energy positron capture works only for the molecules which form bound states with the positron. Secondly, the capture process must involve energy transfer between the electron–positron degrees of freedom and nuclear motion. This means that a positron–molecule complex possesses a complex spectrum of vibrational Feshbach resonances (VFRs).¹ Thirdly, the positron annihilation rate is proportional to the energy *density* of the VFRs populated in the process of capture, rather than to their lifetimes. Finally, for low-energy positrons the capture process can be strongly affected by selection rules and hence depend on the symmetry of the molecule.

Recently direct experimental evidence which links large annihilation rates with molecular vibrations has been obtained [20]. It reveals some details of positron coupling to the vibrationally excited states of the positron–molecule complex. In particular, this work indicates that positron capture by alkanes is enhanced in the vicinity of the C–H vibrational modes. This means that these modes may act as doorways into more complicated molecular vibrations.

There were several calculations of positron–molecule scattering and annihilation, which took

into account molecular vibrations [21]. However, the simple molecules studied have small Z_{eff} . They are unlikely to support positron bound states, and the VFR annihilation mechanism is irrelevant for them. On the other hand, for larger molecules with experimental $Z_{\text{eff}} > 10^3$ the calculations neglecting vibrations strongly underestimate the annihilation rates [22,23].²

In this paper we use a simple zero-range potential model to study the effect of vibrations on positron scattering and annihilation on a dimer, Kr_2 . Kr_2 is a somewhat exotic van der Waals molecule whose binding is ensured by the long-range $-C_6/R^6$ attraction. However, owing to a large equilibrium interatomic distance ($R_0 = 7.56$ a.u. [24]) and weak interaction between the atoms, it is also the system where the zero-range model is more realistic. We will see that with a reasonable choice of parameters this model shows that Kr_2 has a bound positron state and possesses a series of VFRs. The latter gives rise to a strong enhancement of Z_{eff} , as described above.

The zero-range potential model is a standard tool for studying collisional processes [25]. Its use is justified when the problem has two energy scales. For example, when the projectile (positron) energy is small compared to the internal energy of scatterers (atoms). For light-particle scattering it means that the projectile wavenumber k is much smaller than the inverse radius of the scatterer, $k \ll R_{\text{at}}^{-1}$. In this case one can approximate the interaction of the projectile with each scatterer by a boundary condition imposed on the projectile wavefunction at the scatterer. This simplification usually allows one to advance much further analytically and get the answers with a minimal amount of numerical computation. As a result, the underlying physics of the problem remains transparent and a thorough qualitative and, possibly, quantitative understanding can be achieved.

The zero-range approximation was used before to study collision processes involving negative ions, electron–molecule scattering and dissociative

¹ Vibrational Feshbach resonances describe the states of the positron–molecule complex where the positron is bound to the vibrationally excited levels of the molecule in the electronic ground state. They lie below the corresponding vibrational excitation thresholds of the molecule. If the coupling between the light particles (electrons and positron) and nuclear motion were switched off, these resonances would become true bound states. This description of the VFR is in agreement with their understanding in the context of electron–molecule scattering [19].

² To eliminate a computational error the values of Z_{eff} reported in [22] must be divided by Z , the number of electrons in the molecule.

attachment (see, e.g. [26–28]). It was also used recently to model positron binding to methane and its fluorosubstitutes [29].

2. Zero-range model for positron–atom interaction

Let us first consider the interaction of a positron with an isolated Kr atom. As mentioned in Section 1, the dynamics of positron–atom interaction at small distances is characterised by atomic-sized energies. As a result, for a low-energy positron the wavefunction at small distances does not depend on the positron energy, except through a normalisation factor. When the positron is outside the atom the wavefunction of the system is simply a product of the ground-state atomic wavefunction and the positron wavefunction ψ .

This allows one to represent the effect of the interaction between the positron and the atom by a simple boundary condition,

$$\frac{1}{r\psi} \frac{d(r\psi)}{dr} \Big|_{r \rightarrow 0} = -\kappa_0, \quad (2)$$

where κ_0 is a parameter.³ This boundary condition can be integrated to give the asymptotic form of the wavefunction at small r ,

$$\psi \simeq \text{const} \left(\frac{1}{r} - \kappa_0 \right), \quad (3)$$

which is an equivalent form of (2). Of course, the true value of κ_0 can be determined only by doing a full many-body calculation for the positron–atom system.

Outside the atom the positron is free and its s -wave wavefunction is $\psi \propto r^{-1} \sin(kr + \delta_0)$, where k is the momentum (atomic units $\hbar = m_e = |e| = 1$ are used) and δ_0 is the phase-shift. Using this wavefunction in (2) one obtains

³ Boundary condition (2) constitutes the zero-range approximation. The fact that it is set at $r = 0$, rather than at some finite atomic radius R_{at} is justified at low projectile momenta, $kR_{\text{at}} \ll 1$. Indeed, for such k the atomic radius is much smaller than the projectile de Broglie wavelength $\lambda = 2\pi/k$, $R_{\text{at}} \ll \lambda$, and can be considered as “zero”.

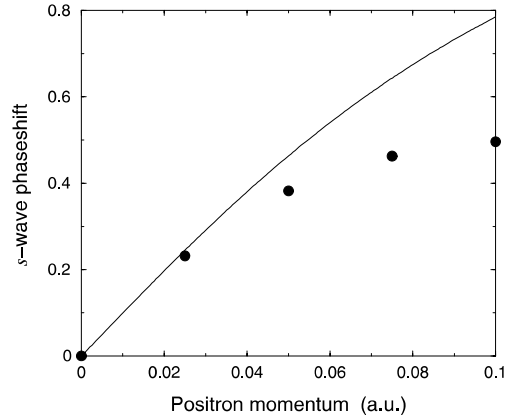


Fig. 1. s -wave phase-shift for positron–Kr scattering. Solid circles are the results of a polarised-orbital calculation [13], solid line is the zero-range model phase-shift, Eq. (4), with $\kappa_0 = -0.1$.

$$\tan \delta_0 = -\frac{k}{\kappa_0} \quad (4)$$

and the s -wave scattering amplitude

$$f \equiv \frac{e^{2i\delta_0} - 1}{2ik} = -\frac{1}{\kappa_0 + ik}. \quad (5)$$

For small momenta $\delta_0 \simeq -k/\kappa_0 \equiv -ak$, where a is the *scattering length* [12], hence the zero-range parameter $\kappa_0 \equiv a^{-1}$. The values of the scattering length for positron on Kr obtained in polarised orbital calculations [13], $a = -10.37$ a.u., and many-body theory calculations [15], $a = -9.1$ a.u., are close. It means that $\kappa_0 = -0.1$ is a reasonable choice for Kr. The applicability of the zero-range approximation at low positron momenta is illustrated by Fig. 1.

Eq. (5) shows that for $k = 0$, $f = -1/\kappa_0 \equiv -a$. Since $|\kappa_0| \ll 1$ a.u. for Kr, the corresponding elastic scattering cross-section at zero energy, $\sigma = 4\pi a^2$, is much larger than the geometric size of the atom. The situation where a is anomalously large negative is usually described by saying that the system has a low-lying virtual s level at the energy $\varepsilon = 1/(2a^2)$ [12]. On the other hand, an anomalously large positive value of a would mean that there is a weakly bound s state. Indeed, for $\kappa_0 > 0$ the amplitude (5) has a pole at the imaginary momentum $k = i|\kappa_0| = i\kappa_0$. The energy

of the bound state is $\varepsilon = k^2/2 = -\kappa_0^2/2$, and the bound-state wavefunction $\psi \propto r^{-1} \exp(-\kappa_0 r)$ satisfies (2).

Positron virtual levels, as well as weakly bound states, lead to enhanced annihilation rates at small positron momenta [11,14]. The zero-range approximation is especially suited for systems with virtual levels or weakly-bound states ($|\kappa_0| \ll R_{\text{at}}$), because many of their properties are determined by the behaviour of the wavefunction outside the target. We will now use this property and develop an approximation which allows one to calculate Z_{eff} using the zero-range positron wavefunction ψ .

It follows from the definition (1) that for a system of Z electrons,

$$Z_{\text{eff}} = \int \sum_{i=1}^Z \delta(\mathbf{r} - \mathbf{r}_i) \times |\Psi_k(\mathbf{r}_1, \dots, \mathbf{r}_Z, \mathbf{r})|^2 d\mathbf{r}_1 \cdots d\mathbf{r}_Z d\mathbf{r}, \quad (6)$$

where \mathbf{r}_i and \mathbf{r} are the coordinates of the electrons and positron, respectively and $\Psi_k(\mathbf{r}_1, \dots, \mathbf{r}_Z, \mathbf{r})$ is the total wavefunction of the system [7,10]. It describes scattering of the positron with initial momentum \mathbf{k} from the atomic or molecular target in the ground state Φ_0 , and is normalised as

$$\Psi_k(\mathbf{r}_1, \dots, \mathbf{r}_Z, \mathbf{r}) \simeq \Phi_0(\mathbf{r}_1, \dots, \mathbf{r}_Z) \left(e^{i\mathbf{k}\cdot\mathbf{r}} + f_{kk'} \frac{e^{i\mathbf{k}\cdot\mathbf{r}}}{r} \right), \quad (7)$$

$r \gg R_{\text{at}},$

where $f_{kk'}$ is the positron scattering amplitude.

As seen from Eq. (6), the annihilation rate is determined by the positron density at the electrons. The latter are mostly confined to the volume of the target. This region is characterised by strong Coulomb interactions between the particles. As a result, for small positron energies ε the wavefunction Ψ inside the target depends on ε only through its normalisation (7). Therefore, it is *proportional* to the scattered positron wavefunction

$$\psi \simeq e^{i\mathbf{k}\cdot\mathbf{r}} + f_{kk'} \frac{e^{i\mathbf{k}\cdot\mathbf{r}}}{r}. \quad (8)$$

Thus, we can write an approximate formula

$$Z_{\text{eff}} = \int \rho(\mathbf{r}) |\psi(\mathbf{r})|^2 d^3\mathbf{r}, \quad (9)$$

where $\rho(\mathbf{r})$ is an *effective* electron density which accounts for the effects of short-range correlations between the annihilating particles.⁴

At small positron energies the scattering is dominated by the *s*-wave. In the zero-range approximation the scattering amplitude is given by Eq. (5) and the wavefunction ψ actually coincides with its asymptotic form (8) at all $r > 0$,

$$\psi = e^{i\mathbf{k}\cdot\mathbf{r}} + f \frac{e^{i\mathbf{k}\cdot\mathbf{r}}}{r}. \quad (10)$$

For $|\kappa_0| \ll R_{\text{at}}$ the second term on the right-hand side of Eq. (10), which represents the scattered wave, is much greater than the first incident-wave term near the target. If we neglect the latter the true radial dependence of the electron density in (9) becomes unimportant, since the result depends on a single parameter $\int \rho(\mathbf{r}) r^{-2} d^3\mathbf{r}$. Mathematically, it is more convenient to introduce the “zero-range electron density”

$$\rho(\mathbf{r}) = \frac{Z_{\text{eff}}^{(0)} \kappa_0^2}{4\pi} \delta(\mathbf{r} - \mathbf{r}_e), \quad r_e \rightarrow 0, \quad (11)$$

and use it in Eq. (9) together with the zero-range wavefunction (10). Taking into account (5), we obtain

$$Z_{\text{eff}} = Z_{\text{eff}}^{(0)} \frac{\kappa_0^2}{\kappa_0^2 + k^2}. \quad (12)$$

In this form it is clear that the parameter $Z_{\text{eff}}^{(0)}$ has the meaning of Z_{eff} at zero positron energy.

It is worth noting that the momentum dependence of $Z_{\text{eff}}(k)$ is the same as that of the zero-range model elastic scattering cross-section

$$\sigma_{\text{el}} = 4\pi |f|^2 = \frac{4\pi}{\kappa_0^2 + k^2}. \quad (13)$$

This is also true in general (i.e. without any model assumptions) for systems with virtual or weakly bound positron states, $|\kappa_0| \ll R_{\text{at}}$, as was first pointed out in [11] (see also [9,10]).

⁴ Such approximation is often used for positron annihilation studies in condensed matter and was applied to positron annihilation on molecules [21]. However, if one neglects short-range correlations and uses the true electron density $\rho(\mathbf{r})$ the value of Z_{eff} is usually grossly underestimated.

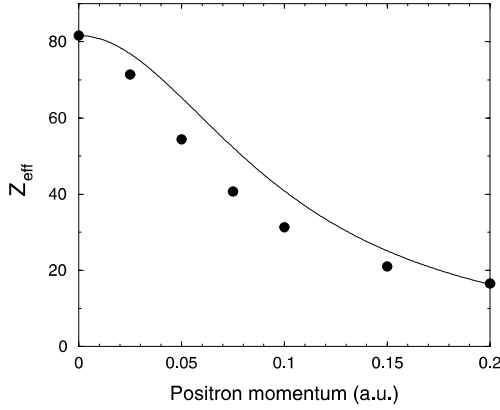


Fig. 2. Z_{eff} in positron collisions with Kr. Solid circles are the results of a polarised-orbital calculation [13], solid line is the zero-range model approximation, Eq. (12), with $\kappa_0 = -0.1$ and $Z_{\text{eff}}^{(0)} = 81.6$.

The applicability of Eq. (12) to positron annihilation on Kr is illustrated in Fig. 2. The value of $Z_{\text{eff}}^{(0)} = 81.6$ is used to match the results of the polarised-orbital calculation [13], which gives Z_{eff} in good agreement with experiment [4,30]. Note that the enhancement of Z_{eff} at small positron momenta and its rapid drop at $k \gtrsim |\kappa_0|$ are directly related to the existence of the positron–Kr virtual level [15].

3. Positron interaction with a molecule

3.1. Wavefunction in the zero-range approximation

Let us consider the interaction of the positron with a diatomic molecule, and let \mathbf{R}_1 and \mathbf{R}_2 be the coordinates of the two atomic nuclei. In the zero-range approximation the positron wavefunction is that of free motion for $\mathbf{r} \neq \mathbf{R}_1, \mathbf{R}_2$. In the scattering problem this wavefunction may contain terms representing the incident positron plane wave and scattered positron spherical waves (cf. Eq. (10)).

Suppose the positron is incident with momentum \mathbf{k}_0 on the dimer in the ground state Φ_0 . The positron–molecule wavefunction outside the atoms can be written in the form of a linear combination with coefficients A_n and B_n [31],

$$\Psi = e^{i\mathbf{k}_0 \cdot \mathbf{r}} \Phi_0(\mathbf{R}) + \sum_n A_n \Phi_n(\mathbf{R}) \frac{e^{i\mathbf{k}_n \cdot |\mathbf{r} - \mathbf{R}_1|}}{|\mathbf{r} - \mathbf{R}_1|} + \sum_n B_n \Phi_n(\mathbf{R}) \frac{e^{i\mathbf{k}_n \cdot |\mathbf{r} - \mathbf{R}_2|}}{|\mathbf{r} - \mathbf{R}_2|}, \quad (14)$$

where \mathbf{k}_0 is the incident positron momentum, Φ_n is the n th (vibrational) state of the molecule, and $\mathbf{R} = \mathbf{R}_1 - \mathbf{R}_2$ is the interatomic distance. The two sums on the right-hand side represent scattering events which leave the molecule in the n th excited state, and \mathbf{k}_n is the corresponding positron momentum (see below).

It is easy to check that the wavefunction (14) satisfies the Schrödinger equation

$$\left[-\frac{1}{2} \Delta_{\mathbf{r}} - \frac{1}{2\mu} \Delta_{\mathbf{R}} + U(\mathbf{R}) \right] \Psi = \left(\frac{k_0^2}{2} + E_0 \right) \Psi, \quad (15)$$

where μ is the reduced mass of the atoms, $U(\mathbf{R})$ is the molecular potential energy, E_0 is its ground-state energy, Φ_n are the eigenstates of the molecular Hamiltonian,

$$\left[-\frac{1}{2\mu} \Delta_{\mathbf{R}} + U(\mathbf{R}) \right] \Phi_n(\mathbf{R}) = E_n \Phi_n(\mathbf{R}), \quad (16)$$

and the positron momenta obey energy conservation

$$\frac{k_0^2}{2} + E_0 = \frac{k_n^2}{2} + E_n. \quad (17)$$

The channels with $E_n - E_0 < k_0^2/2$ are open and the corresponding momenta $k_n = [k_0^2 - 2(E_n - E_0)]^{1/2}$ are real. For closed channels, $E_n - E_0 > k_0^2/2$, the momenta are imaginary, $k_n = i[k_0^2 - 2(E_n - E_0)]^{1/2}$, and the corresponding exponents in Eq. (14) do not contribute to the outgoing positron wave.

Note that in (15) we neglect the terms produced by the action of the nuclear kinetic-energy operator on the wavefunction of the light particle, since they are suppressed by the large atomic mass μ .

In what follows we also neglect the effect of rotation of the molecule and assume that the atoms move along a fixed straight line. In the low-energy collision processes of interest the positron wavefunction is dominated by the s -wave. This means that the angular momentum of the molecule

is unlikely to change during the collision.⁵ Given that molecular rotation is a slow process we can consider the molecular axis as fixed.

The wavefunction (14) must satisfy the zero-range boundary condition (3) at each of the two atoms, $\mathbf{R}_{1,2} = \pm \mathbf{R}/2$ (choosing the origin at the centre of mass),

$$\Psi|_{r \rightarrow R_i} \simeq \text{const} \left(\frac{1}{|r - \mathbf{R}_i|} - \kappa_0 \right). \quad (18)$$

Multiplying the resulting equation by $\Phi_n^*(\mathbf{R})$ and integrating over the nuclear coordinates, one obtains a set of linear equations for the coefficients A_n and B_n ,

$$(\kappa_0 + ik_n)A_n + \sum_m \left(\frac{e^{ik_m R}}{R} \right)_{nm} B_m = -(e^{ik_0 n R/2})_{n0}, \quad (19)$$

$$(\kappa_0 + ik_n)B_n + \sum_m \left(\frac{e^{ik_m R}}{R} \right)_{nm} A_m = -(e^{-ik_0 n R/2})_{n0}, \quad (20)$$

where \mathbf{n} is a unit vector along the molecular axis, $(\dots)_{nm}$ are matrix elements between molecular vibrational states, e.g.

$$(e^{ik_0 n R/2})_{n0} = \int \Phi_n^*(R) e^{ik_0 n R/2} \Phi_0(R) dR, \quad (21)$$

and the wavefunctions $\Phi_n(R)$ are solutions of the one-dimensional Schrödinger equation

$$\left[-\frac{1}{2\mu} \frac{d^2}{dR^2} + U(R) \right] \Phi_n(R) = E_n \Phi_n(R). \quad (22)$$

Eqs. (19) and (20) yield the coefficients A_n and B_n which determine the scattering wavefunction (14) and all observable quantities (see Section 3.2).

For an arbitrary molecular potential $U(R)$ the wavefunctions $\Phi_n(R)$ and matrix elements which appear in Eqs. (19) and (20) have to be found numerically. However, if we use the harmonic approximation the matrix elements involving mo-

lecular vibrational states can be evaluated analytically, see Appendix A.

3.2. Cross-sections and Z_{eff}

The wavefunction (14) at large positron–molecule separations contains the positron plane wave incident on the ground-state molecule, and a sum of outgoing spherical waves in the *open* channels,

$$\Psi \simeq e^{ik_0 r} \Phi_0(\mathbf{R}) + \sum_n f_n(\mathbf{n}') \frac{e^{ik_n r}}{r} \Phi_n(\mathbf{R}), \quad (23)$$

where

$$f_n(\mathbf{n}') = A_n e^{-ik_n \mathbf{n}' \cdot \mathbf{R}_0/2} + B_n e^{ik_n \mathbf{n}' \cdot \mathbf{R}_0/2} \quad (24)$$

is the amplitude of elastic ($n = 0$) or inelastic vibrational excitation ($n > 0$) scattering, \mathbf{n}' is a unit vector in the direction of the final-state positron momentum and $\mathbf{R}_0 = \mathbf{n}R_0$.

The total elastic ($n = 0$) and vibrational excitation cross-sections are obtained by integration over the directions of the scattered positron,

$$\sigma_{0 \rightarrow n} = \frac{k_n}{k_0} \int |f_n|^2 d\mathbf{n}' \approx 4\pi \frac{k_n}{k_0} |A_n + B_n|^2, \quad (25)$$

the last expression being valid at low positron momenta, $k_n R_0 < 1$, when the cross-section is isotropic.

The positron annihilation rate for the molecule is found by calculating the overlap of the positron density $|\Psi(\mathbf{r})|^2$ with the electron densities at both atoms (cf. Eq. (9)), and integrating over the atomic as well as positron coordinates,

$$Z_{\text{eff}} = \int [\rho(\mathbf{r} - \mathbf{R}/2) + \rho(\mathbf{r} + \mathbf{R}/2)] |\Psi(\mathbf{r})|^2 d^3 r d\mathbf{R}. \quad (26)$$

Using Eq. (14) and the “zero-range densities” (11), one obtains

$$Z_{\text{eff}} = Z_{\text{eff}}^{(0)} \kappa_0^2 \sum_n (|A_n|^2 + |B_n|^2), \quad (27)$$

where the sum over n here includes both open and closed channels, unlike that in Eq. (23), because the annihilation takes place at the target and not at $r \rightarrow \infty$.

⁵ Note that this approximation may not be good for molecules with permanent dipole moments. A charged particle (positron) interacts with a dipole by means of a long-range $1/r^2$ potential, which mixes the projectile partial waves and causes transitions between different rotational states of the molecule.

3.3. Bound states

The existence of a bound state on a single zero-range centre is determined by the sign of κ_0 (Section 2), and $\kappa_0 < 0$, as for the positron on Kr, means that there is no bound state.

However, when the two non-binding centres are sufficiently close to each other the positron may form a bound state with the dimer. For example, in the fixed-nuclei approximation the positron bound-state wavefunction in the zero-range approximation should have the form

$$\Psi_0 = A \frac{e^{-\kappa|r-R_0/2|}}{|r-R_0/2|} + B \frac{e^{-\kappa|r+R_0/2|}}{|r+R_0/2|}. \quad (28)$$

Subjecting it to boundary conditions (18) leads to a set of two linear homogeneous equations for A and B . (Since $A = B$ for the lowest eigenstate of a diatomic molecule built of identical atoms, it is enough to use only one boundary condition.) It has a non-zero solution if κ satisfies the transcendental equation [33]

$$\kappa = \kappa_0 + \frac{e^{-\kappa R_0}}{R_0}. \quad (29)$$

Its positive solution corresponds to the bound state with the energy $\varepsilon = -\kappa^2/2$. Eq. (29) has such solution for $\kappa_0 < 0$ if $R_0 < -1/\kappa_0$.

For example, $\kappa_0 = -0.1$ for Kr means that two Kr atoms bind the positron if the interatomic distance is smaller than 10 a.u. Given the Kr_2 equilibrium distance of $R_0 = 7.56$ a.u. we conclude that according to the zero-range model a stable $e^+\text{Kr}_2$ complex does exist.

To go beyond the fixed-nuclei approximation one should consider a wavefunction similar to Eq. (14) without the incident-wave term and apply boundary conditions (18) to it. This wavefunction must be considered at negative positron energies $\varepsilon = -\kappa^2/2$, corresponding to imaginary momenta $k_0 = i|k_0| \equiv i\kappa$ and $k_n = i|k_n|$.

Instead of deriving a new set of equations one may simply recall that according to the general theory of scattering, the scattering amplitude has poles at the energies of the bound states [12]. Therefore, one can find the positions of the bound states by looking for poles of A_n and B_n from Eqs. (19) and (20) at negative projectile energies.

4. Results

4.1. Parameters of the model

To apply the zero-range model developed in Section 3 to positron interaction with Kr_2 we must first specify the parameters of the model. The interaction of the positron with each of the Kr atoms is described by $\kappa_0 = -0.1$ and $Z_{\text{eff}}^{(0)} = 81.6$ (see Section 2).

The recommended values of the equilibrium distance and potential minimum depth for the Kr_2 molecule are $R_0 = 7.56$ a.u. and $U(R_0) = -17.2$ meV, respectively [24], and its reduced mass is $\mu = 7.64 \times 10^4$ a.u. To find the vibrational frequency ω , the interatomic potential has been approximated by a sum of the short-range electron-exchange repulsion term and the long-range van der Waals attraction,

$$U(R) = BR^z e^{-\beta R} - \left(\frac{C_6}{R^6} + \frac{C_8}{R^8} + \frac{C_{10}}{R^{10}} \right) f_c(R). \quad (30)$$

The latter is multiplied by a cut-off function $f_c(R)$ which cancels the $1/R^n$ divergence at small distances,

$$f_c(R) = \theta(R - R_c) + \theta(R_c - R) e^{-(R_c/R-1)^2}, \quad (31)$$

where $\theta(x)$ is the unit step function: $\theta(x) = 1$ for $x > 0$, $\theta(x) = 0$ for $x < 0$. The values of the

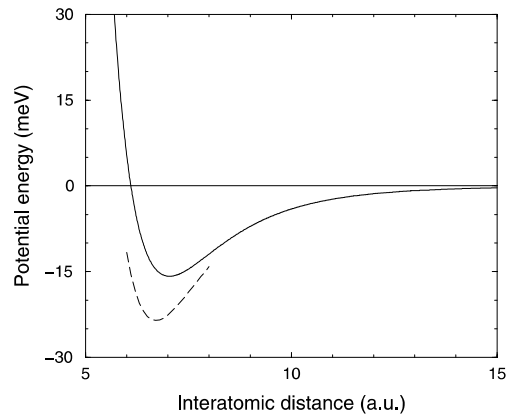


Fig. 3. Approximate molecular potential curves for Kr_2 , $U(R)$ of Eq. (30) (solid line) and $e^+\text{Kr}_2$ (dashed line). The latter is obtained by adding the fixed-nuclei positron binding energy $\varepsilon(R) = -\kappa^2/2$ to $U(R)$.

parameters in atomic units are $B = 6.1$, $\alpha = 2.30$, $\beta = 2.06$, $C_6 = 130$, $C_8 = 2700$ and $C_{10} = 7 \times 10^4$ [24]. A cut-off radius of $R_c = 13$ a.u. provides a reasonable description of the minimum with $R_0 \approx 7$ a.u., see Fig. 3. The second derivative at the minimum $U'' = 6.11 \times 10^{-3}$ a.u. yields the vibrational frequency $\omega = \sqrt{U''/\mu} = 8.9 \times 10^{-5}$ a.u. = 2.42 meV = 19.5 cm⁻¹. Besides R_0 and μ , ω is the only molecular parameter needed to do calculations in the harmonic approximation [34].

4.2. Bound states

In the fixed-nuclei approximation the positron binding energy on Kr₂ is found from Eq. (29). For $R = R_0$ it gives $\kappa = 0.0166$, $\varepsilon = -\kappa^2/2 = -3.75$ meV. This energy is greater than ω , which means that positron binding may be accompanied by vibrational excitation of the positron–molecule complex (see below).

Eq. (29) allows one to find the binding energy as a function of R . The sum $U(R) + \varepsilon(R)$ represents the adiabatic potential curve of $e^+\text{Kr}_2$. Fig. 3 shows that its minimum is shifted towards smaller R . A closer inspection reveals that the second derivative at the minimum has become smaller, which means that $e^+\text{Kr}_2$ has a lower vibrational frequency ω' than its parent molecule.

The positron–Kr₂ binding energy with account of the nuclear motion is found by searching for poles of A_n and B_n at imaginary $k_0 = ik$. The set of linear equations (19) and (20) and the number of coefficients A_n and B_n are, strictly speaking, infinite. For doing numerical calculations the set of equations can be truncated by assuming that $A_n = B_n = 0$ for $n > N_c$. This means that only the first $N_c + 1$ channels with $n = 0, 1, \dots, N_c$ are taken into consideration. Note that if Eqs. (19) and (20) are truncated at $N_c = 0$ they become equivalent to the fixed-nuclei approximation.

Practically, the value of N_c should be sufficiently large to ensure that the results do not change upon its further increase. From a physical point of view such truncation is possible because the coupling of higher vibrational excitations is very small (see Appendix A). For the calculations reported in this paper N_c values up to 15 have been used.

Using the parameters listed in Section 4.1 we find that the scattering amplitude has poles at $\kappa = 0.0182$, 0.0130 and 0.0029. These values correspond to three bound states with energies

$$\begin{aligned} \varepsilon_0 &= -4.51 \text{ meV}, & \varepsilon_1 &= -2.30 \text{ meV} & \text{and} \\ \varepsilon_2 &= -0.11 \text{ meV}. \end{aligned} \quad (32)$$

The lowest of these states lies deeper than that obtained in the fixed-nuclei approximation at the Kr₂ equilibrium distance (−3.75 meV), because allowing the nuclei to move leads to stabilisation. Indeed, as we have seen from Fig. 3, the minimum of the $e^+\text{Kr}_2$ potential curve, $U(R) + \varepsilon(R)$, is shifted towards smaller distances compared to $U(R)$. Using the adiabatic potential curves, the true binding energy of the $e^+\text{Kr}_2$ complex can be estimated as follows:

$$[U(R) + \varepsilon(R)]_{\min} - U_{\min} + \frac{\omega'}{2} - \frac{\omega}{2} \approx \varepsilon_0,$$

where we have also included the ground-state vibrational energies of $e^+\text{Kr}_2$ and Kr₂.

The two higher energies, ε_1 and ε_2 , describe vibrationally excited bound states of the positron–molecule complex, and the energy difference

$$\varepsilon_{n+1} - \varepsilon_n \approx 2.20 \text{ meV} \quad (33)$$

corresponds to the vibrational frequency ω' of $e^+\text{Kr}_2$. As mentioned above, it is smaller than that of Kr₂.

Higher vibrational excitations of $e^+\text{Kr}_2$ do not represent bound states. They are embedded in the positron–Kr₂ continuum and correspond to positron–molecule VFRs. They manifest themselves in the scattering cross-sections and positron annihilation rate (see below). The term “Feshbach resonance” applies to those quasibound states whose decay is due to coupling between different degrees of freedom of the system. In our case the higher vibrational excitations of $e^+\text{Kr}_2$ would be stable if the energy of the vibrational motion could not be transferred to the positron. Of course, the same coupling is responsible for the capture of the continuous-spectrum positron into these vibrationally excited states of the $e^+\text{Kr}_2$ complex. Using (32) and (33) we can predict that VFRs should be observed at positron energies $\varepsilon \approx 2.1, 4.3, 6.5, \dots$ meV.

4.3. Scattering

Fig. 4 shows the elastic and vibrational excitation cross-sections obtained from Eq. (25). In the fixed-nuclei approximation (dashed line) the shape and magnitude of the elastic scattering cross-section is determined by the existence of the weakly bound positron state with $\kappa = 0.0166$ (Section 3.3),

$$\sigma \approx \frac{4\pi}{\kappa^2 + k^2},$$

cf. Eq. (13). When the nuclear motion is taken into account by solving Eqs. (19) and (20) for a large number of channels N_c , the cross-sections show strong VFR features at positron energies

$$\varepsilon = \varepsilon_0 + n\omega' \quad (n = 3, 4, 5).$$

The figure shows that each scattering channel is coupled most strongly with the lowest VFR occurring above the channel threshold. This is a consequence of the weak positron-vibrational coupling. Another manifestation of this weakness is a hierarchy of magnitudes of the cross-sections, $\sigma_{0 \rightarrow n+1} \ll \sigma_{0 \rightarrow n}$.

A feature also worth mentioning is a prominent rise of the elastic cross-section $\sigma_{0 \rightarrow 0}$ towards zero

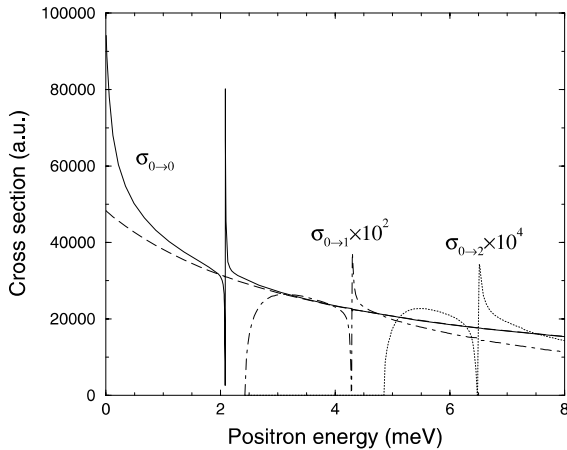


Fig. 4. Cross-sections for positron scattering from Kr_2 : elastic scattering cross-section in the fixed-nuclei approximation (dashed line) and with account of nuclear motion ($\sigma_{0 \rightarrow 0}$, solid line); vibrational excitation cross-sections $\sigma_{0 \rightarrow 1}$ (chain line) and $\sigma_{0 \rightarrow 2}$ (dotted line) are shown multiplied by 10^2 and 10^4 , respectively.

positron energy. It is caused by the presence of the weakly bound $n = 2$ state with $\varepsilon_2 = -0.11$ meV just below the threshold.

4.4. Annihilation

The VFRs feature even more prominently in the positron annihilation rate, Fig. 5. Note that to show the magnitude Z_{eff} at the resonant peaks as well as the non-resonant background a logarithmic Z_{eff} scale has to be used. Thus, the peak value of the first strongest resonance is $Z_{\text{eff}} = 1.1 \times 10^7$, four orders of magnitude above the background.

Fig. 6 shows the resonances in detail. By fitting Breit–Wigner profiles to the numerical Z_{eff} over the resonances,

$$Z_{\text{eff}} \propto \frac{1}{(\varepsilon - \varepsilon_n)^2 + \Gamma^2/4}, \quad (34)$$

we determine their positions and widths,

$$\varepsilon_3 = 2081.8 \text{ } \mu\text{eV}, \quad \Gamma = 3.5 \text{ } \mu\text{eV},$$

$$\varepsilon_4 = 4285.7 \text{ } \mu\text{eV}, \quad \Gamma = 15 \text{ } \mu\text{eV}.$$

As a consequence of weak positron-vibrational coupling, the resonances are narrow, compared to the spacing between them. The second resonance is, though, much wider and lower than the first one. Since its energy is above the first inelastic

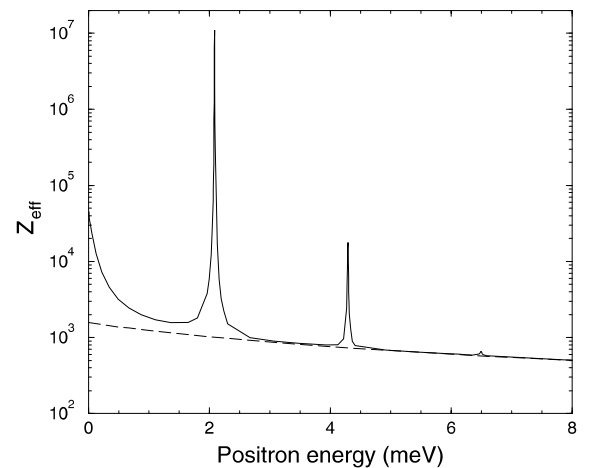


Fig. 5. Z_{eff} for positrons on Kr_2 in the fixed-nuclei approximations (dashed line) and with account of the nuclear motion (solid line).

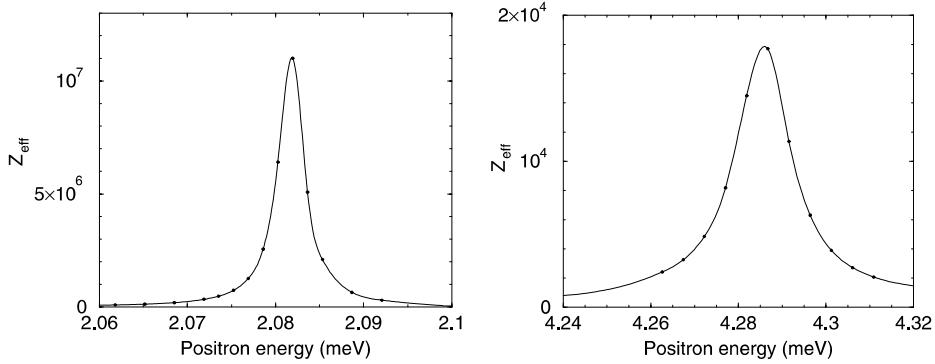


Fig. 6. Vibrational Feshbach resonances $n = 3$ and 4 in Z_{eff} for positrons on Kr_2 . Dots are values of Z_{eff} found numerically and solid lines show Breit–Wigner profile fits, $Z_{\text{eff}} \propto [(\varepsilon - \varepsilon_n)^2 + \Gamma^2/4]^{-1}$, which allow one to determine the positions and widths of the resonances.

threshold, it decays by positron emission leading to the molecular ground and first excited states ($0 \rightarrow 0$ and $0 \rightarrow 1$ scattering channels). This is one of the reasons why the $n = 4$ resonance has a larger width.

Of course, when the resonances are so narrow it is unclear whether they would affect any observed Z_{eff} if the positrons are not monoenergetic, e.g. have a certain energy spread $\Delta\varepsilon$. A simple estimate can be obtained by smearing the contribution of the strongest $n = 3$ resonance over the vibrational spacing ω' . This suppresses its magnitude by a factor $\Gamma/\omega' \sim 10^{-3}$, which means that the resonant contribution is still an order of magnitude greater than the background $Z_{\text{eff}} \sim 10^3$.

Theoretically, the contribution of an s -wave resonance to the annihilation rate is given by

$$\Delta Z_{\text{eff}}^{(\text{res})} = \frac{\pi}{k} \frac{\Gamma_e}{(\varepsilon - \varepsilon_n)^2 + \Gamma^2/4} \frac{\Gamma_a}{\pi r_0^2 c}, \quad (35)$$

where Γ_e is the so-called elastic width, Γ_a is the annihilation width and $\Gamma = \Gamma_e + \Gamma_a$ is the total width [9,10,12]. This formula is valid for a resonance below the first inelastic (vibrational) threshold. For higher-lying resonances the total width must also include an additional contribution due to positron emission accompanied by the vibrational excitation of the target.

When Z_{eff} is calculated by means of Eq. (6) it is assumed that the annihilation cross-section is much smaller than that of elastic scattering. In other words, the annihilation rate is calculated

perturbatively, using the scattering wavefunction Ψ which is found neglecting annihilation. Applied to resonances, this means that the contribution of annihilation to the resonance width is neglected. This is true when $\Gamma_a \ll \Gamma_e$ or $\Gamma \approx \Gamma_e$. It is easy to check that this condition is fulfilled in the present calculation. Comparing Eq. (35) to the numerical data for the $n = 3$ resonance, we obtain $\Gamma_a \sim 0.05 \mu\text{eV} \ll \Gamma$. A similar estimate of the annihilation width Γ_a is also obtained from the zero-range bound-state wavefunction, see Appendix B.

Note that in the regime where $\Gamma \approx \Gamma_e$ the integral contribution of the resonance $\int \Delta Z_{\text{eff}}^{(\text{res})} d\varepsilon$ is independent of Γ , i.e. its contribution does not depend on the strength of positron coupling to vibrations. This means that although the resonance is very narrow it is also very tall ($\propto \Gamma^{-1}$), and its contribution to Z_{eff} is substantial (see below).

Note also that the last of the bound states situated just below threshold at $\varepsilon_2 = -0.11 \text{ meV}$, causes a rapid rise of Z_{eff} at $\varepsilon \rightarrow 0$. It can be thought of as being due to virtual capture of a continuous-spectrum positron into a weakly bound state. Similarly to Eq. (35), its contribution is proportional to $1/(\varepsilon - \varepsilon_2)^2$.

4.5. Annihilation for thermal positrons

All positron annihilation experiments except the most recent one, Ref. [20], were done with thermalised positrons. It is, therefore, useful to

average Z_{eff} over the Maxwellian momentum distribution of the positrons,

$$\bar{Z}_{\text{eff}}(T) = \int_0^\infty \frac{e^{-k^2/2k_B T}}{(2\pi k_B T)^{3/2}} Z_{\text{eff}}(k) 4\pi k^2 dk, \quad (36)$$

and present it as a function of positron temperature T , Fig. 7. At very low temperatures, $k_B T \ll \varepsilon_n$, the $n = 3$ Feshbach resonance does not contribute to the annihilation rate. However, as soon as the high-energy tail of the Maxwellian distribution overlaps with the resonance, Z_{eff} shows a rapid onset of the resonant contribution. Note that this happens at temperatures well below $k_B T \approx \varepsilon_n$, where the contribution of the resonance to $\bar{Z}_{\text{eff}}(T)$ is maximal. The resonance also continues to contribute strongly for $k_B T > \varepsilon_n$. Consider, for example, the annihilation rate at room temperatures, $k_B T = 25$ meV, which is 10 times the energy of the $n = 3$ resonance. Here the fixed-nuclei result is $\bar{Z}_{\text{eff}} = 250$, the contribution of the non-resonant background from the full coupled calculation is similar, $\bar{Z}_{\text{eff}} = 270$, but taking into account the resonance increases the annihilation rate to $\bar{Z}_{\text{eff}} = 1000$ (see Fig. 7).

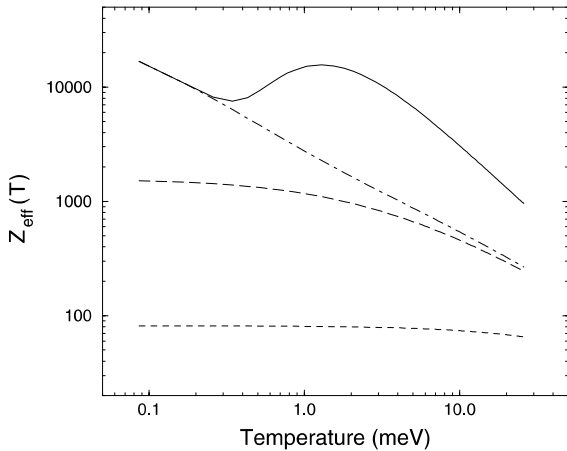


Fig. 7. Thermally averaged Z_{eff} for positrons on Kr_2 : fixed-nuclei approximation (long-dashed line); with account of nuclear motion, non-resonant background (chain line), and including the contribution of the vibrational Feshbach resonance (solid line). For comparison Z_{eff} for Kr is shown by short-dashed line.

5. Summary and outlook

The zero-range potential model has been used to investigate positron binding, scattering and annihilation for a simple diatomic molecule, Kr_2 . In this approximation the system is described by a small number of parameters which characterise the Kr_2 molecule (R_0 and ω in the harmonic approximation), and positron interaction and annihilation with individual Kr atoms (κ_0 and $Z_{\text{eff}}^{(0)}$). The model allows deep analytical treatment. Supplemented by simple numerical calculations, it produces a rich and “life-like” physical picture of positron–molecule interaction.

The main facets of this picture are: (i) ground and vibrationally excited positron–molecule bound states, (ii) vibrational Feshbach resonances observed in elastic and vibrationally inelastic scattering, and most importantly, (iii) very strong enhancement of the annihilation rate due to these resonances.

To the best of my knowledge, the present calculation is the first dynamical calculation of positron–molecule collisions which confirms the role of binding and capture in vibrational Feshbach resonances for positron–molecule annihilation.

As far as the actual numerical results for Kr_2 are concerned, the values presented above may certainly be affected by the choice of parameters. Thus, in the absence of precise positron–Kr calculations it is impossible to argue that $\kappa_0 = -0.1$ is the true value to be used. The approximations made in deriving the zero-range model may also affect the quantitative results. From this point of view the present work aims at showing *how* things happen when positrons interact with molecules, rather than making firm predictions for a particular system.

There are some other effects that one can investigate using the zero-range model. For example, one can calculate the vibrational eigenstates numerically using the molecular potential curve. This will allow one to check the validity and limitations of the the harmonic approximation. One can also study molecular dissociation by positrons, or dissociation into a neutral atom and positive ion, which may follow the annihilation.

It should also be possible to apply the zero-range model to positron interaction with “normal” molecules rather than the weakly bound van der Waals species. However, the results of such modelling will probably be more qualitative than quantitative, because the use of the zero-range approximation is harder to justify for them. On the other hand, owing to its simplicity, the zero-range approximation may allow one to attack larger polyatomic molecules. This is where the current interest in positron annihilation on molecules lies.

Appendix A. Matrix elements in the harmonic approximation

Near the equilibrium the molecular potential can be expanded as

$$U(R) \simeq U_{\min} + \frac{\mu\omega^2}{2}(R - R_0)^2, \quad (\text{A.1})$$

where μ is the mass and ω is the vibrational frequency of the corresponding harmonic oscillator. In this approximation the wavefunctions $\Phi_n(R)$ are given by the eigenstates $\chi_n(R - R_0)$ of the harmonic oscillator with energies $E_n = \omega(n + \frac{1}{2})$ for $n = 0, 1, \dots$. The matrix elements are then calculated as follows:

$$\begin{aligned} (e^{i\mathbf{k}_0 \cdot \mathbf{n}R/2})_{n0} &= e^{i\mathbf{k}_0 \cdot \mathbf{n}R_0/2} \int \Phi_n(R) e^{i\mathbf{k}_0 \cdot \mathbf{n}(R-R_0)/2} \Phi_0(R) dR \\ &= e^{i\mathbf{k}_0 \cdot \mathbf{n}R_0/2} \left(\frac{\mu\omega}{2^k \pi k!} \right)^{1/2} \\ &\quad \times \int_{-\infty}^{\infty} e^{-\mu\omega x^2} e^{i\lambda x} H_n(\sqrt{\mu\omega}x) dx, \quad (\text{A.2}) \end{aligned}$$

where $x = R - R_0$ is the displacement from the equilibrium, $\lambda = \mathbf{k}_0 \cdot \mathbf{n}/2$, and we used an explicit expression of the oscillator eigenstates in terms of Hermite polynomials H_n [12]. Calculating the standard integral in Eq. (A.2) [32], we obtain

$$\begin{aligned} (e^{i\mathbf{k}_0 \cdot \mathbf{n}R/2})_{n0} &= e^{i\mathbf{k}_0 \cdot \mathbf{n}R_0/2} \frac{1}{\sqrt{n!}} \left(\frac{i\mathbf{k}_0 \cdot \mathbf{n}}{2\sqrt{2\mu\omega}} \right)^n \\ &\quad \times \exp \left[-\frac{(\mathbf{k}_0 \cdot \mathbf{n})^2}{16\mu\omega} \right]. \quad (\text{A.3}) \end{aligned}$$

The quantity $(\mu\omega)^{-1/2}$ is the classical amplitude of vibrations in the ground state. This amplitude for a molecule is much smaller than the low-energy positron de Broglie wavelength, therefore $k_0(\mu\omega)^{-1/2} \ll 1$. This means that the exponent in Eq. (A.3) is very close to unity and the matrix element drops rapidly with n . This also allows one to calculate the matrix elements *in the leading order* very quickly using the fact that for an oscillator the non-zero matrix elements of the displacement are [12]

$$x_{n,n-1} = x_{n-1,n} = \sqrt{\frac{n}{2\mu\omega}}. \quad (\text{A.4})$$

As a result, for a small parameter $\lambda \ll (\mu\omega)^{-1/2}$,

$$\begin{aligned} (e^{i\lambda x})_{n0} &\simeq \left(\frac{(i\lambda x)^n}{n!} \right)_{n0} \\ &= x_{n,n-1} x_{n-1,n-2} \cdots x_{2,1} x_{1,0} (i\lambda)^{n/n!} \\ &= \frac{1}{\sqrt{n!}} \left(\frac{i\lambda}{\sqrt{2\mu\omega}} \right)^n, \quad (\text{A.5}) \end{aligned}$$

which immediately leads to (A.3) with $\exp(\dots) \simeq 1$.

Evaluation of the second matrix element

$$\left(\frac{e^{i\mathbf{k}_m R}}{R} \right)_{nm} = \int \Phi_n^*(R) \frac{e^{i\mathbf{k}_m R}}{R} \Phi_m(R) dR \quad (\text{A.6})$$

is done similarly. Expanding in powers of $x = R - R_0$ and rearranging the sums, we obtain

$$\begin{aligned} \frac{e^{i\mathbf{k}_m R}}{R} &= \frac{e^{i\mathbf{k}_m R_0}}{R_0} \frac{e^{i\mathbf{k}_m x}}{1 + x/R_0} \\ &= \frac{e^{i\mathbf{k}_m R_0}}{R_0} \sum_{k=0}^{\infty} (-1)^k \left(\frac{x}{R_0} \right)^k \sum_{l=0}^{\infty} \frac{(i\mathbf{k}_m x)^l}{l!} \\ &= \frac{e^{i\mathbf{k}_m R_0}}{R_0} \sum_{N=0}^{\infty} \left[\sum_{l=0}^N \frac{(-i\mathbf{k}_m R_0)^l}{l!} \right] \left(-\frac{x}{R_0} \right)^N. \quad (\text{A.7}) \end{aligned}$$

Following (A.5), we see that only $N = |n - m|$ contributes to the matrix element in the leading order, hence

$$\left(\frac{e^{ik_m R}}{R}\right)_{nm} = \frac{e^{ik_m R_0} (-1)^{|n-m|}}{R_0 (R_0 \sqrt{2\mu\omega})^{|n-m|}} \sqrt{\frac{\max(n, m)!}{\min(n, m)!}} \times \sum_{l=0}^{|n-m|} \frac{(-ik_m R_0)^l}{l!}. \quad (\text{A.8})$$

Appendix B. Annihilation rate in the positron–molecule bound state

For fixed nuclei the annihilation rate in the bound state is (cf. Eqs. (1) and (26))

$$\Gamma_a = \pi r_0^2 c \int [\rho(\mathbf{r} - \mathbf{R}_0/2) + \rho(\mathbf{r} + \mathbf{R}_0/2)] |\Psi_0(\mathbf{r})|^2 d^3 r,$$

where Ψ_0 is the bound-state wavefunction (28). Using the zero-range electron densities (11) and normalisation

$$\int |\Psi_0(\mathbf{r})|^2 d^3 r = 1, \quad (\text{B.1})$$

which yields

$$A = B = \left[\frac{\kappa}{4\pi(1 + e^{-\kappa R_0})} \right]^{1/2}, \quad (\text{B.2})$$

we obtain

$$\Gamma_a = \pi r_0^2 c \frac{Z_{\text{eff}}^{(0)} \kappa_0^2 \kappa}{2\pi(1 + e^{-\kappa R_0})}, \quad (\text{B.3})$$

where κ is related to the energy of the bound state $\varepsilon = -\kappa^2/2$. Note that for $\kappa R_0 \ll 1$

$$\Gamma_a \propto \sqrt{|\varepsilon|},$$

which is generally true for weakly bound states, as shown in [10,35].

Applying Eq. (B.3) to the lowest positron–Kr₂ bound state, $\kappa = 0.0182$, we obtain $\Gamma_a = 0.04 \mu\text{eV}$, in agreement with the estimate obtained from $\Delta Z_{\text{eff}}^{(\text{res})}$ in Section 4.4. Of course, it should be possible to derive a more accurate formula for Γ_a than Eq. (B.3), by going beyond the fixed-nuclei approximation (see end of Section 3.3). However, it is natural that the annihilation rate in the bound or quasibound (VFR) state does not depend much on the state of the nuclear motion.

References

- [1] M. Deutsch, Phys. Rev. 83 (1951) 866.
- [2] D.A.L. Paul, L. Saint-Pierre, Phys. Rev. Lett. 11 (1963) 493.
- [3] S.J. Tao, Phys. Rev. Lett. 14 (1965) 935.
- [4] G.R. Heyland, M. Charlton, T.C. Griffith, G.L. Wright, Can. J. Phys. 60 (1982) 503.
- [5] C.M. Surko, A. Passner, M. Leventhal, F.J. Wysocki, Phys. Rev. Lett. 61 (1988) 1831.
- [6] K. Iwata, R.G. Greaves, T.J. Murphy, M.D. Tinkle, C.M. Surko, Phys. Rev. A 51 (1995) 473, and references therein; see also Koji Iwata, Positron annihilation on atoms and molecules, Ph.D. Dissertation, University of California, San Diego, 1997.
- [7] P.A. Fraser, Adv. At. Mol. Phys. 4 (1968) 63.
- [8] T.J. Murphy, C.M. Surko, Phys. Rev. Lett. 67 (1991) 2954.
- [9] G.F. Gribakin, Phys. Rev. A 61 (2000) 022720.
- [10] G.F. Gribakin, in: C.M. Surko, F.A. Gianturco (Eds.), New Directions in Antimatter Chemistry and Physics, Kluwer Academic Publishers, Dordrecht, 2001, p. 413.
- [11] V.I. Goldanskii, Yu.S. Sayasov, Phys. Lett. 13 (1964) 300.
- [12] L.D. Landau, E.M. Lifshitz, Quantum Mechanics, third ed., Pergamon, Oxford, 1977.
- [13] R.P. McEachran, A.G. Ryman, A.D. Stauffer, J. Phys. B 12 (1979) 1031; R.P. McEachran, A.D. Stauffer, L.E.M. Campbell, J. Phys. B 13 (1980) 1281.
- [14] V.A. Dzuba, V.V. Flambaum, W.A. King, B.N. Miller, O.P. Sushkov, Phys. Scripta T 46 (1993) 248.
- [15] V.A. Dzuba, V.V. Flambaum, G.F. Gribakin, W.A. King, J. Phys. B 29 (1996) 3151.
- [16] P.M. Smith, D.A.L. Paul, Can. J. Phys. 48 (1970) 2984.
- [17] G.K. Ivanov, Dokl. Akad. Nauk SSSR 291 (1986) 622; Dokl. Phys. Chem. 291 (1986) 1048.
- [18] O.H. Crawford, Phys. Rev. A 49 (1994) R3147.
- [19] A. Schramm, I.I. Fabrikant, J.M. Weber, E. Leber, M.-W. Ruf, H. Hotop, J. Phys. B 32 (1999) 2153.
- [20] S.J. Gilbert, L.D. Barnes, J.P. Sullivan, C.M. Surko, Phys. Rev. Lett. 88 (2002) 043201.
- [21] F.A. Gianturco, T. Mukherjee, Europhys. Lett. 48 (1999) 519; F.A. Gianturco, T. Mukherjee, Nucl. Instr. and Meth. B 171 (2000) 17.
- [22] E.P. da Silva, J.S.E. Germane, M.A.P. Lima, Phys. Rev. Lett. 77 (1996) 1028; E.P. da Silva et al., Nucl. Instr. and Meth. B 143 (1998) 140; C.R.C. de Carvalho et al., Nucl. Instr. and Meth. B 171 (2000) 33; M.T. do N. Varella, C.R.C. de Carvalho, M.A.P. Lima, Nucl. Instr. and Meth. B 192 (2002) 225.
- [23] F.A. Gianturco, T. Mukherjee, T. Nishimura, A. Occhigrossi, in: C.M. Surko, F.A. Gianturco (Eds.), New Directions in Antimatter Chemistry and Physics, Kluwer Academic Publishers, Dordrecht, 2001, p. 451;

- F.A. Gianturco, T. Mukherjee, T. Nishimura, A. Occhigrossi, Phys. Rev. A 64 (2001) 032715.
- [24] A.A. Radtsig, B.M. Smirnov, Parameters of Atoms and Atomic Ions: Handbook, Energoatomizdat, Moscow, 1986.
- [25] Yu.N. Demkov, V.N. Ostrovsky, Zero-Range Potentials and Their Applications in Atomic Physics, Plenum Press, New York, 1988.
- [26] A.Z. Devdariani, Zh. Tekh. Fiz. 43 (1973) 399; Sov. Phys. – Tech. Phys. 18 (1973) 255.
- [27] G.F. Drukarev, I.Y. Yurova, J. Phys. B 10 (1977) 3551.
- [28] J.P. Gauyacq, J. Phys. B 13 (1980) 4417; J.P. Gauyacq, J. Phys. B 15 (1982) 2721; A. Herzenberg, J.P. Gauyacq, J. Phys. B 17 (1984) 1155.
- [29] K. Iwata, G.F. Gribakin, R.G. Greaves, C. Kurz, C.M. Surko, Phys. Rev. A 61 (2000) 022719.
- [30] C. Kurz, R.G. Greaves, C.M. Surko, Phys. Rev. Lett. 77 (1996) 2929.
- [31] E.E. Nikitin, B.M. Smirnov, Atomic and Molecular Processes, Nauka, Moscow, 1988.
- [32] I.S. Gradshteyn, I.M. Ryzhik, Table of Integrals, Series, and Products, Academic Press, London, 1980.
- [33] B.M. Smirnov, O.B. Firsov, Sov. Phys. JETP 20 (1965) 156.
- [34] This value is close to the recommended $\omega = 24.1 \text{ cm}^{-1}$ from K.P. Huber, G. Herzberg, Constants of Diatomic Molecules, van Nostrand Reinhold, New York, 1979.
- [35] J. Mitroy, I.A. Ivanov, Phys. Rev. A, accepted for publication.